

# mRNA Encoding a Bispecific Single Domain Antibody Construct Protects against Influenza A Virus Infection in Mice

Lien Van Hoecke,<sup>1,2</sup> Rein Verbeke,<sup>3,4</sup> Dorien De Vlieger,<sup>1,5</sup> Heleen Dewitte,<sup>3,4,6</sup> Kenny Roose,<sup>1,5</sup> Sharon Van Nevel,<sup>7</sup> Olga Krysko,<sup>7</sup> Claus Bachert,<sup>7</sup> Bert Schepens,<sup>1,2,5</sup> Ine Lentacker,<sup>3,4</sup> and Xavier Saelens<sup>1,5</sup>

<sup>1</sup>VIB-UGent Center for Medical Biotechnology, VIB, 9000 Ghent, Belgium; <sup>2</sup>Department of Biomedical Molecular Biology, Ghent University, 9000 Ghent, Belgium; <sup>3</sup>Laboratory of General Biochemistry & Physical Pharmacy, Ghent University, 9000 Ghent, Belgium; <sup>4</sup>Cancer Research Institute Ghent, 9000 Ghent, Belgium; <sup>5</sup>Department of Biochemistry and Microbiology, Ghent University, 9000 Ghent, Belgium; <sup>6</sup>Laboratory for Molecular and Cellular Therapy, Vrije Universiteit Brussel, 1090 Jette, Belgium; <sup>7</sup>Upper Airways Research Laboratory, Department of Head and Skin, Ghent University, 9000 Ghent, Belgium

**To date, mRNA-based biologics have mainly been developed for prophylactic and therapeutic vaccination to combat infectious diseases or cancer. In the past years, optimization of the characteristics of *in vitro* transcribed mRNA has led to significant reduction of the inflammatory responses. Thanks to this, mRNA therapeutics have entered the field of passive immunization. Here, we established an mRNA treatment that is based on mRNA that codes for a bispecific single-domain antibody construct that can selectively recruit innate immune cells to cells infected with influenza A virus. The constructs consist of a single-domain antibody that binds to the ectodomain of the conserved influenza A matrix protein 2, while the other single-domain antibody binds to the activating mouse Fcγ receptor IV. Formulating the mRNA into DOTAP (1,2-dioleoyl-3-trimethylammonium-propane)/cholesterol nanoparticles and delivering these intratracheally to mice allowed the production of the bispecific single-domain antibody in the lungs, and administration of these mRNA-particles prior to influenza A virus infection was associated with a significant reduction in viral titers and a reduced morbidity in mice. Overall, our data provide evidence that the local delivery of mRNA encoding a bispecific single-domain antibody format in the lungs could be a promising pulmonary antiviral prophylactic treatment.**

## INTRODUCTION

In the nineties, Wolff et al.<sup>1</sup> showed that exogenous transcribed mRNA can be used to express proteins *in vivo*. However, only in recent years, mRNA has emerged as a promising drug platform technology. So far, *in vitro* transcribed (IVT) mRNA has shown its utility as a vaccine format in cancer immunotherapy<sup>2–5</sup> and as a tool to promote prophylactic protection against infectious diseases.<sup>5–10</sup> A number of modifications to the vector used to produce the mRNA, as well as to the synthetic mRNA itself, have further ameliorated the biologic properties of the IVT mRNA. For example, modified nucleotides such as N1-methylpseudouridine (N1mΨ) are used to decrease inappropriate stimulation of cellular RNA sensors and, thus, to avoid a strong

induction of pro-inflammatory cytokine secretion. As the potency and safety of mRNA treatments grew, other fields of application for mRNA-based biologics became accessible. These include the application of mRNA encoding different antibody formats to protect against different viral, bacterial, or malignant diseases.<sup>11–14</sup>

The use of mRNA for passive immunization has several benefits compared to the use of recombinant proteins. For instance, mRNA is produced in cell-free circumstances and because it consists of only four building blocks, it has uniform physicochemical properties. These characteristics enable a safe and generic production and purification process, potentially reducing the costs compared to a protein-based approach. Additionally, mRNA can give rise to protein expression for a few days, leading to prolonged and higher peak titers of the antibody format in circulation compared with the protein format. This is of interest as it entails that with mRNA the frequency of dose administration could be reduced. On top, monoclonal antibodies are prone to a wide variety of post-translational modifications, including glycosylation, deamidation, oxidation, incomplete disulfide bond formation, N-terminal glutamine cyclization, and C-terminal lysine processing. The use of mRNA encoding antibodies allows for the *in situ* production of the biologics in the body itself. Also, problems of purification and heterogeneity of the end product can be circumvented.

Single domain antibodies (VHHs, also known as nanobodies), derived from the variable domain of heavy-chain-only antibodies found in camelids, have been used in many therapeutic applications.<sup>15</sup> Recently, our group developed a novel anti-influenza A virus strategy based on an engineered bispecific VHH construct that is able to selectively recruit innate immune cells to influenza A virus-infected cells.<sup>16</sup>

Received 18 February 2020; accepted 27 April 2020;  
<https://doi.org/10.1016/j.omtn.2020.04.015>.

**Correspondence:** Xavier Saelens, VIB-UGent Center for Medical Biotechnology, VIB, 9000 Ghent, Belgium.

**E-mail:** [xavier.saelens@vib-ugent.be](mailto:xavier.saelens@vib-ugent.be)



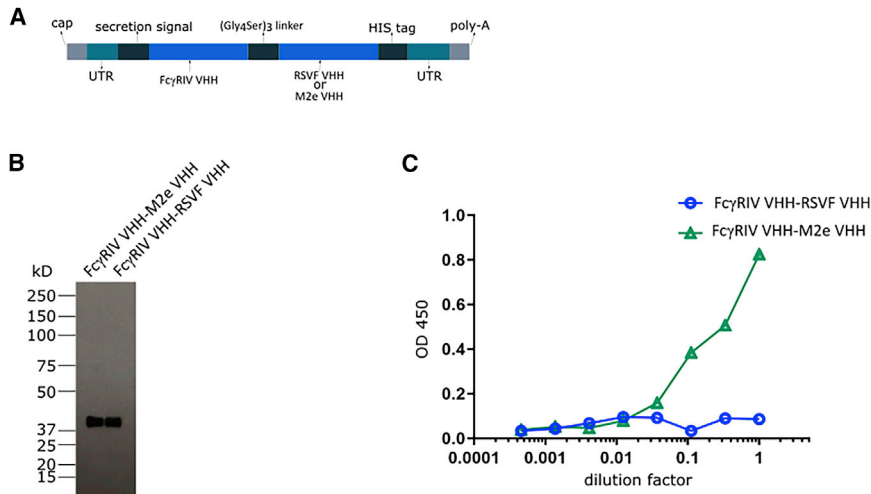


**Figure 1. *In Vitro* Characterization of mRNA Encoded Bispecific VHH Constructs**

(A) Design of mRNA encoding the bispecific VHH constructs (RiboBiFEs). The two VHHs that are genetically linked by means of a flexible 15 amino acid residues long (Gly<sub>4</sub>Ser)<sub>3</sub> linker are directed to the secretory pathway by a secretion signal derived from the murine Ig heavy chain V region BCL1 precursor. The VHH fusion constructs also contain a His<sub>6</sub>-tag at the carboxy-terminus. Two types of RiboBiFEs were constructed: M2e VHH linked to Fc $\gamma$ RIV VHH or RSVF VHH (directed against the fusion protein of respiratory syncytial virus) linked to Fc $\gamma$ RIV VHH. (B) Immunoblot detection with a His<sub>6</sub>-tag-specific horseradish peroxidase (HRP)-conjugated antibody of the medium fraction of mRNA transfected HEK293T cells. HEK293T cells were transfected with 10  $\mu$ g of IVT mRNA coding for the indicated His<sub>6</sub>-tagged RiboBiFEs. 48 h later, one tenth of the trichloroacetic acid precipitated supernatant was analyzed by non-reducing western

blot analysis. (C) The ability of the mRNA encoding Fc $\gamma$ RIV VHH-M2e VHH and the Fc $\gamma$ RIV VHH-RSVF VHH to bind to M2e was investigated in an M2e peptide ELISA. Supernatants from HEK293T cells 48 h after transfection with mRNA encoding the RiboBiFEs were used.

This was accomplished by genetically linking a VHH that binds with moderate affinity to the conserved influenza A matrix protein 2 ectodomain (M2e) to a VHH that specifically binds to the mouse Fc $\gamma$  receptor IV (Fc $\gamma$ RIV). By administering these bispecific VHH antibodies 4 h before and 20 h after influenza A virus infection, morbidity caused by an influenza A virus challenge could be significantly lowered. The M2e is chosen as a target as it is highly conserved among different influenza A subtypes, and different murine studies have shown that M2e-based vaccines can induce a broad protection that is antibody mediated.<sup>17–19</sup> It is shown that alveolar macrophages are the main cell types that are responsible for protection by anti-M2e antibodies.<sup>20</sup> M2 is expressed on the surface of cells infected with influenza A virus. Therapeutic administration of a human M2e-specific immunoglobulin G1 (IgG1) monoclonal antibody was associated with reduced symptoms compared with placebo treatment in a controlled human influenza virus challenge model.<sup>21,22</sup> Fc $\gamma$ Rs are expressed on different innate immune cells like macrophages, neutrophils, natural killer cells, and dendritic cells.<sup>23,24</sup>

Here, we propose the use of *in vitro* transcribed nucleoside-modified mRNA coding for the engineered bispecific VHH construct. We generated N1-methylpseudouridine-containing mRNAs encoding His-tagged bispecific VHH (RiboBiFE; bispecific Fc-receptor engaging) of which one part is directed against M2e and the other part against the mouse Fc $\gamma$ RIV. For the pulmonary delivery of the RiboBiFE constructs, the low-immunogenic nucleoside-modified mRNA was formulated in a liposomal formulation composed of the cationic lipid DOTAP (1,2-dioleoyl-3-trimethylammonium-propane) and cholesterol. We found that the intratracheal (i.t.) administration of mRNA-DOTAP/cholesterol nanoparticles in mice resulted in an expression of the bispecific VHH construct in the lungs, with detectable protein expression levels for at least 2 days. Furthermore, with a single shot of mRNA-nanoparticles encoding the RiboBiFE

construct before an influenza A virus challenge, we could significantly lower morbidity and pulmonary virus titers. These findings further underline the merit of mRNA-based strategies in passive immunization settings.

## RESULTS

### Design and *In Vitro* Characterization of RiboBiFEs

Here, we designed a mRNA-treatment based on the recent report of De Vlioger et al.<sup>16</sup> on a protein bispecific VHH fusion construct consisting of a VHH moiety selectively binding to the activating mouse Fc $\gamma$ RIV and another VHH moiety that binds to the conserved influenza A M2e domain. A flexible 15 amino acid residues long (Gly<sub>4</sub>Ser)<sub>3</sub> linker was used to genetically fuse the two VHH moieties. Upstream of the VHHs a secretion signal derived from the Ig heavy chain V region BCL1 precursor was added and an His<sub>6</sub>-tag was included at the carboxy-terminus. To increase translation efficiency and half-life of the mRNA, we flanked the coding sequence by optimized untranslated regions (UTRs). From this construct we generated N1-methylpseudouridine (m1 $\Psi$ )-containing mRNAs encoding the bispecific VHH constructs, which we termed RiboBiFEs (Figure 1A). As a negative control, RiboBiFEs comprising the Fc $\gamma$ RIV-VHH linked to a VHH directed against the respiratory syncytial virus fusion protein (Fc $\gamma$ RIV VHH-RSVF VHH) were constructed.

The expression of intact *in vitro* transcribed (IVT) RiboBiFEs was confirmed by a western blot analysis on the trichloroacetic acid precipitated supernatant of HEK293T cells transfected with the RiboBiFEs (Figure 1B). Next, we evaluated whether the *in situ* produced protein derived from the RiboBiFE-format is still able to bind to its M2e target as reported by De Vlioger et al.<sup>16</sup> Using an M2e peptide enzyme-linked immunosorbent assay (ELISA), we confirmed the ability of the Fc $\gamma$ RIV VHH-M2e VHH RiboBiFE to bind to its M2e target (Figure 1C).

### I.t. Administration of mRNA Encoding Bispecific VHHs Using DOTAP/Cholesterol Nanoparticles

In previous reports by Verbeke et al.,<sup>25,26</sup> mRNA nanoparticles composed of DOTAP and cholesterol were developed and characterized for the systemic delivery of mRNA vaccines. Due to electrostatic interactions, cationic DOTAP/cholesterol liposomes form complexes with negatively charged mRNA, protecting the mRNA cargo from degradation and holding stable transfection efficiencies *in vivo*. To obtain an efficient mRNA expression of the RiboBiFE construct at the viral entry site, we investigated in this study whether we could use this lipid formulation for the pulmonary delivery of mRNA via i.t. instillation.

The positively charged mRNA nanoparticles are expected to interact with noncellular components present in the lungs, such as phospholipids and proteins, which may affect physicochemical and functional properties of the nanoformulation. Therefore, we first analyzed the colloidal stability of the mRNA nanoparticles in bronchoalveolar lavage fluid (BALF). After 1 h incubation in BALF, the mRNA nanoparticles displayed a 1.85-fold increase in size going from 183 nm to 339 nm, indicating a reduction in colloidal stability in presence of biomolecular lung content.

Next, we evaluated the mRNA delivery efficiency in BALB/c mice after i.t. administration of mRNA nanoparticles, using different reporter mRNAs, as well by the inclusion of a lipophilic, near-infrared fluorescent dye DiR inside the liposome formulation. In a first experiment, mice were instilled with DOTAP/cholesterol particles containing 5 µg of luciferase reporter mRNA. 6 h post administration, a selective and evenly distributed luciferase expression, was detected in the lungs (Figure 2B). In a second experiment, mice were administered with nanoparticles containing both DiR dye and mCherry reporter mRNA. These mRNA nanoparticles allowed us to identify which pulmonary cell types were involved in the uptake of mRNA particles, as well as to evaluate the mRNA translation in each cell type. For this, transfected lungs of mice were collected at 6 h or 24 h post administration, and the different pulmonary cells subsets were analyzed by flow cytometry for the presence of DiR signal and mCherry expression. At 6 h, nanoparticle uptake was detected in CD45<sup>+</sup> immune cells with a percentage of 3.5% ± 1.7% nanoparticle-positive cells, which increased up to 5.3% ± 2.3% by 24 h (Figure 2C). In contrast, almost no DiR signal was detected in the CD45<sup>-</sup> (nonimmune) cell population (0.12% ± 0.06%). When looking in more detail at the cellular uptake in pulmonary immune cell subsets, it appeared that alveolar macrophages were primarily responsible for the clearance of the particles, with a percentage of 43.8% ± 24.8% nanoparticle-positive alveolar macrophages at 6 h and 65.5% ± 27.3% at 24 h. There were no significant levels of DiR signal detected in the other cell subsets (Figure 2D). With respect to the expression of mCherry mRNA, we found a cell-specific mRNA translation in alveolar macrophages with a transfection efficiency of 19.9% ± 10.9% mCherry-positive cells at 6 h and 31.5% ± 17.9% at 24 h (Figure 2E). Finally, to determine the kinetics and durability specific for the expression of the therapeutic mRNA construct, a single

dose of mRNA particles composed with the FcγRIV VHH-M2e VHH RiboBiFE construct was delivered i.t. to the lungs of BALB/c mice. BALF was taken 6, 24, or 48 h after i.t. instillation. Using M2e-peptide ELISA, the highest expression was seen 6 h post administration followed by a gradual decrease but retaining detectable levels up to 48 h after instillation (Figure 2F; Figure S2). We compared the absolute antibody titers after injection of the mRNA-particles with the antibody titers obtained after i.t. instillation of 50 µg of the bispecific FcγRIV VHH-M2e VHH fusion protein as performed by De Vlieger et al.<sup>16</sup> BALF was taken 24 or 48 h after i.t. instillation and absolute titer was determined. Only 24 h after instillation of the bispecific protein, antibody titers above the detection limit were detected (Figure 2F; Figure S2).

Taken together, these results demonstrate that the i.t. administration of DOTAP/cholesterol mRNA nanoparticles can achieve a local and durable expression of the (RiboBiFE) mRNA in the lungs, with a cell specific uptake and mRNA translation by alveolar macrophages.

### Acute Inflammatory Responses to i.t. Instilled mRNA Nanoparticles

In the mice that were i.t. instilled with the reporter mRNA nanoparticles containing mCherry mRNA and DiR dye, we also screened for inflammatory responses that may be triggered by the lipid formulation itself, as well as by innate immune reactions to the mRNA cargo. For this, we first investigated whether the mRNA nanoparticles activated the recruitment of inflammatory cells to the lungs, which could indicate the presence of acute lung inflammation. Overall, the infiltration of CD45<sup>+</sup> cells, as well as most of the specific immune cell subsets that we evaluated, were not subject to changes in their relative abundance in the lung. Only a temporary increase in the levels of granulocytes (gated out as CD11c<sup>-</sup>, MHC-II<sup>-</sup>, CD11b<sup>+</sup>, CD24<sup>+</sup> cells) was observed, which was restored to baseline values within 24 h (Figure 3A). In terms of systemic cytokine responses generated by the i.t. instilled mRNA nanoparticles, we measured a panel of 13 inflammatory cytokines and chemokines (Figure 3B). We could detect a higher concentration of interleukin-6 (IL-6) in the blood samples at 6 h post administration of mRNA nanoparticles, which again returned to baseline by 24 h. Other than for IL-6, no statistically significant differences were observed for the other investigated cytokines and chemokines relative to PBS-treated mice.

### Evaluation of the Protective Potential of Pulmonary Delivery of RiboBiFEs in an Influenza A Virus Infection

Previously, De Vlieger et al.<sup>16</sup> demonstrated that bispecific FcγRIV VHH-M2e VHH fusion protein, recombinantly produced in *Pichia pastoris*, could protect mice from body weight loss and lethality caused by an influenza A virus infection when 50 µg of the protein was administered intranasal 4 h before and 20 h after infection. In accordance, we investigated the potential of the mRNA encoded FcγRIV VHH-M2e VHH RiboBiFEs to protect in a similar influenza challenge model *in vivo*. To this end, 5 µg m1-Ψ modified mRNA complexed into DOTAP/cholesterol particles was administered i.t. 4 h before challenge with 2 × LD<sub>50</sub> of X47 (H3N2) influenza A virus.

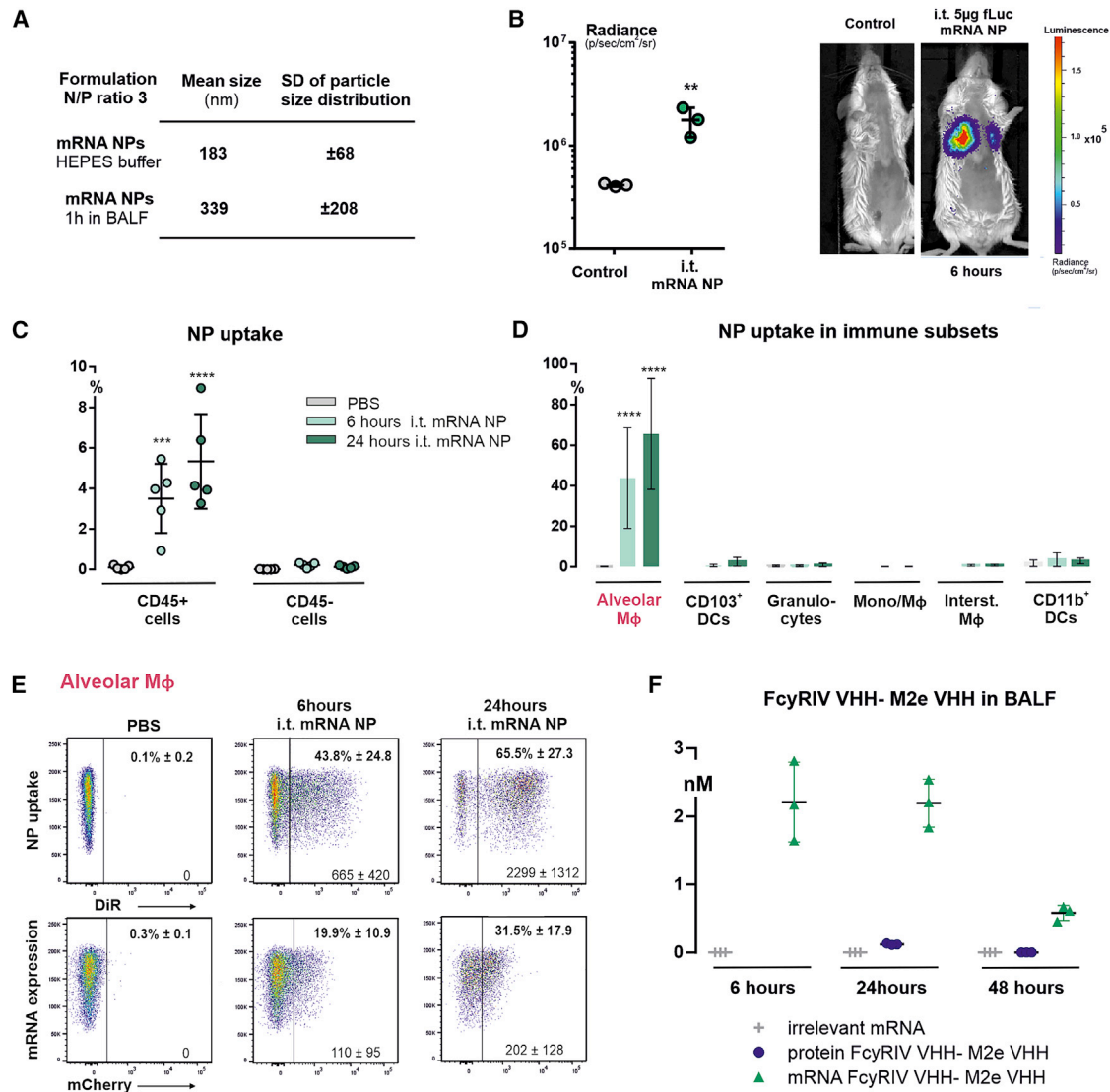


**Figure 2. Delivery of DOTAP/Cholesterol mRNA Lipid Nanoparticles via Intratracheal Instillation**

(A) Particle size analysis after incubating DOTAP/cholesterol mRNA lipoplexes in HEPES buffer or bronchoalveolar lavage fluid (BALF). BALB/c mice were i.t. administered with DOTAP/cholesterol particles formulated with different mRNA sequences (mRNA dose of 5  $\mu$ g). (B) Graph and representative whole-body images showing expression levels of luciferase mRNA (5-methoxyuridine) in lungs of BALB/c mice measured via bioluminescence imaging at 6 h ( $n = 3$  mice). DOTAP/cholesterol nanoparticles containing 1 mol% of the lipophilic dye DiR and packaged with mCherry mRNA (5-methoxyuridine) were i.t. administered, after which nanoparticle uptake (DiR fluorescence) and mRNA expression (mCherry protein) were evaluated in a variety of pulmonary cells subsets ( $n = 5$  mice) at 6 and 24 h post administration. The flow cytometry gating strategy used to discriminate between pulmonary immune cell subsets can be found in the Figure S1 and was adopted from Knight et al.<sup>45</sup> PBS-instilled mice serve as negative controls. (C) Graph shows nanoparticle uptake in CD45 positive cells (immune cells) and CD45 negative cells (nonimmune cells). (D) Nanoparticle uptake in a variety of pulmonary immune cells subsets, including alveolar macrophages, CD103<sup>+</sup> dendritic cells (CD103<sup>+</sup>DCs), granulocytes, other subsets of monocytes and macrophages that are not encompassed by the other subsets (Mono/macrophage), interstitial macrophages, and CD11b<sup>+</sup> DCs. (E) Representative flow cytometry plots of nanoparticle uptake and mCherry mRNA expression in alveolar macrophages. The mean percentage of DiR-positive and mCherry-positive cells, together with the mean fluorescence intensity of each signal, are given in each flow plot. (F) 5  $\mu$ g of Fc $\gamma$ RIV VHH-M2e VHH or Fc $\gamma$ RIV VHH-RSVF VHH (irrelevant mRNA) formulated in DOTAP/cholesterol particles or 50  $\mu$ g Fc $\gamma$ RIV VHH-M2e VHH protein was instilled i.t. in BALB/c mice. 6, 24, or 48 h after instillation, BALF was isolated and cells were removed from the BALF and the ability of His<sub>6</sub>-tagged proteins to bind to M2e was investigated in a peptide ELISA (see Figure S2). De absolute titers were calculated using the standard curve shown in Figure S2. Graphs show mean  $\pm$  SEM ( $n = 3$  mice per group). Statistical analyses on datasets were performed by one-way ANOVA followed by Tukey's post hoc test. Asterisks indicate statistical significance compared to negative control (\* $p < 0.05$ ; \*\* $p < 0.01$ ; \*\*\* $p < 0.001$ ; \*\*\*\* $p < 0.0001$ ).



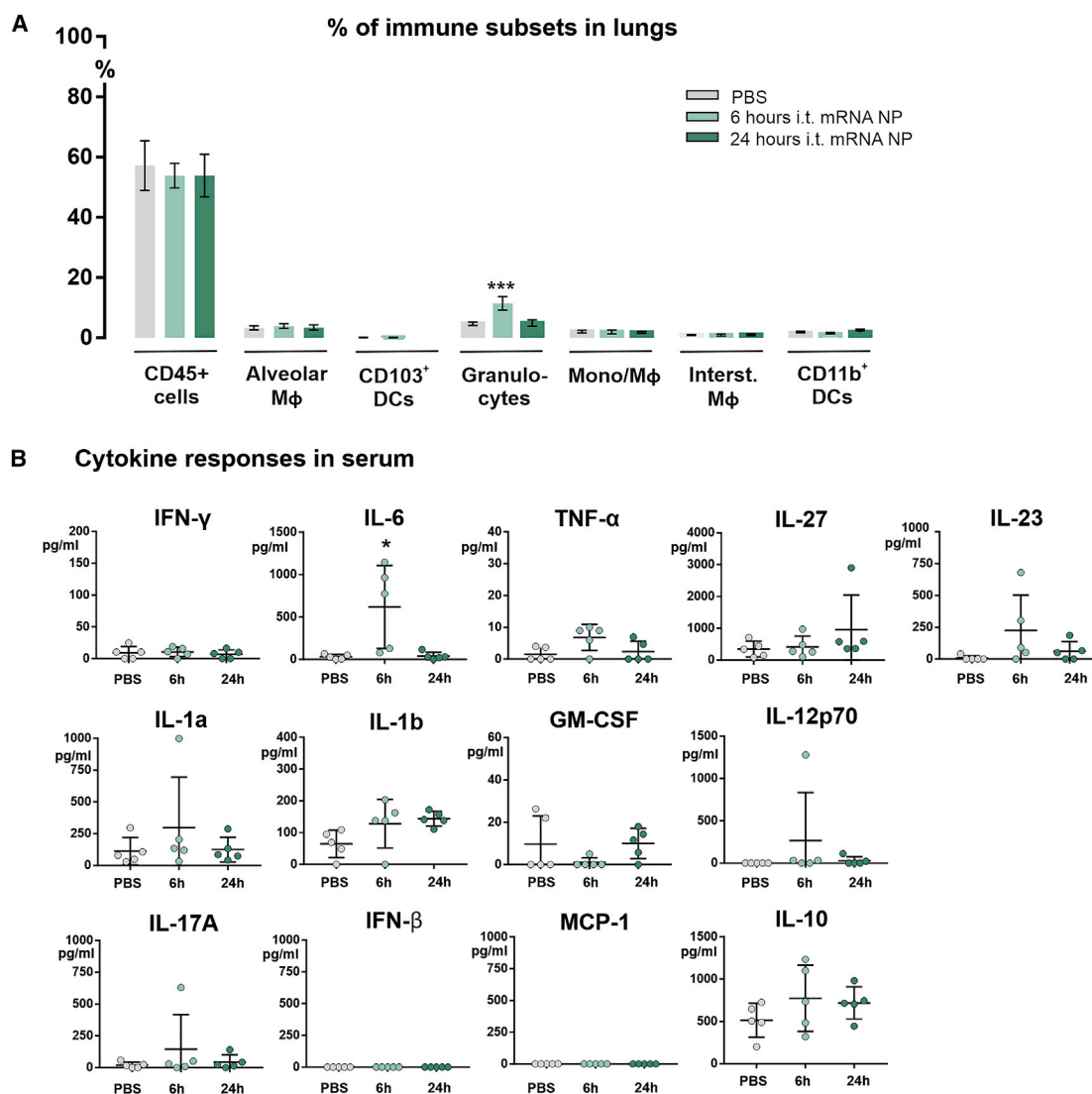


**Figure 3. Inflammatory Response to Intratracheally Administered mRNA Nanoparticles**

(A) Graph depicts the relative distribution of each pulmonary immune cell subset as a percent of total viable cells, for PBS-treated mice, and mice that were i.t. instilled with DiR-labeled mRNA nanoparticles containing mCherry mRNA (mRNA dose of 5  $\mu$ g), that were either sacrificed at 6 or 24 h post administration ( $n = 5$  mice). (B) Serum samples collected from these mice were screened for the presence of inflammatory cytokine responses. Statistical analyses on datasets were performed by one-way ANOVA followed by Tukey's post hoc test. Asterisks indicate statistical significance compared to negative control (\* $p < 0.05$ ; \*\*\* $p < 0.001$ ).

As controls, mice were treated with PBS or nanoparticles containing luciferase mRNA or non-influenza targeted Fc $\gamma$ RIV VHH-RSVF VHH mRNA. Body weight change and mortality were monitored daily after virus challenge. Mice that had been treated with Fc $\gamma$ RIV VHH-M2e VHH RiboBiFEs were significantly better protected from body weight loss and lethality caused by the influenza virus infection compared to the negative control groups (Figure 4A). A subset of the treated mice was euthanized on day 6 after challenge to determine the pulmonary virus titers after treatment and infection using plaque assay. Analysis showed that the protection mediated by Fc $\gamma$ RIV VHH-M2e VHH RiboBiFE was associ-

ated with a statistically significant reduction in lung viral titer (Figure 4B).

Finally, we verified whether the protection by the Fc $\gamma$ RIV VHH-M2e VHH RiboBiFE was indeed mediated by Fc $\gamma$ RIV engagement. For this, wild-type and Fc $\gamma$ RIV<sup>-/-</sup> C57BL/6 mice were i.t. treated with 5  $\mu$ g of mRNA encoding Fc $\gamma$ RIV VHH-M2e VHH or as negative control mRNA encoding luciferase or Fc $\gamma$ RIV VHH-RSVF VHH. 4 h later, mice were intranasally challenged with  $2 \times LD_{50}$  of A/X47 (H3N2) influenza virus. Treatment with mRNA encoding Fc $\gamma$ RIV VHH-M2e VHH was able to protect wild-type mice against the

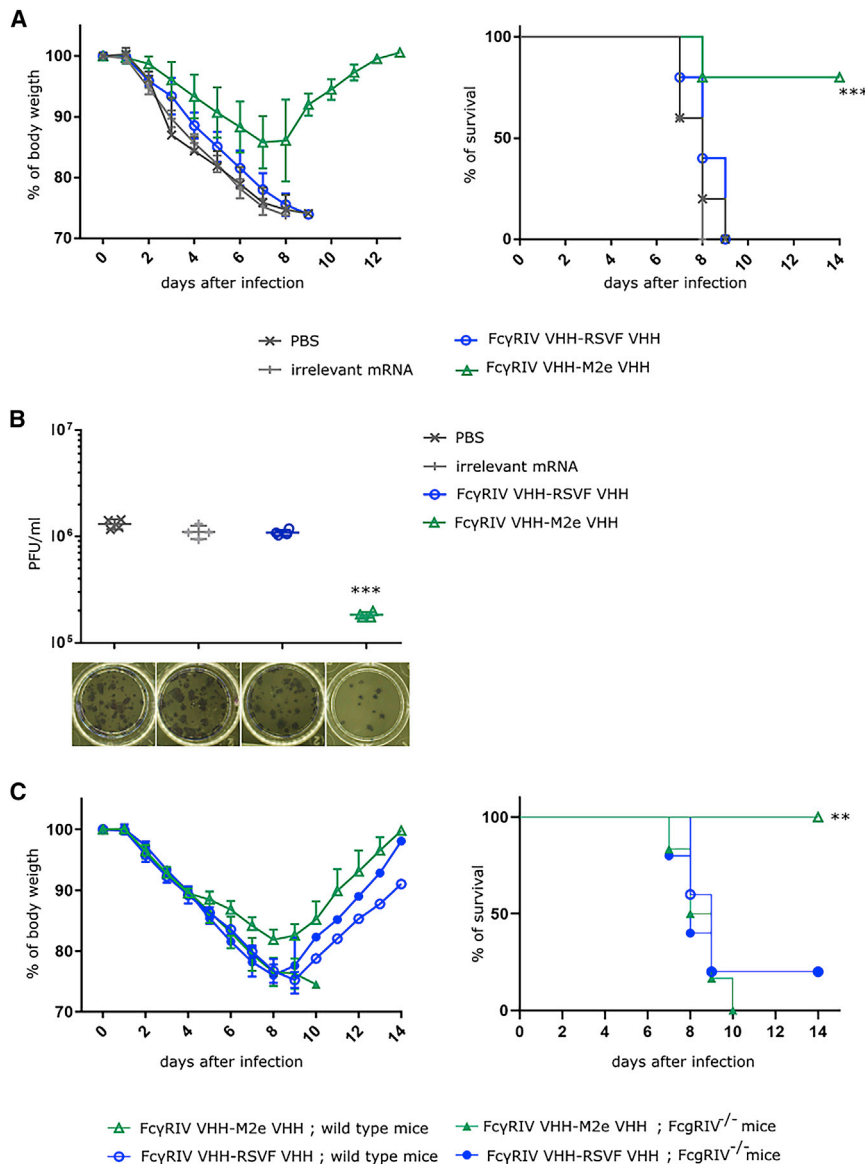


**Figure 4. In Vivo Delivery of Lipid Nanoparticle Formulated mRNA that Encode Fc $\gamma$ RIV VHH-M2e VHH Protects Mice against a Potentially Lethal Influenza A Virus Challenge**

(A) BALB/c mice were i.t. instilled with PBS or 5  $\mu$ g mRNA encoding Fc $\gamma$ RIV VHH-M2e VHH, Fc $\gamma$ RIV VHH-RSVF VHH, or luciferase (irrelevant) mRNA formulated in DOTAP/cholesterol particles. 4 h later, mice were challenged with 2 $\times$  LD<sub>50</sub> of A/X47 (H3N2) influenza virus. Body weight change (left) and survival (right) were monitored for 14 days. The mean relative changes in body weight together with their standard errors are represented. The survival rate of the group receiving RiboBiFEs encoding Fc $\gamma$ RIV VHH-M2e VHH was significantly different from the control groups (\*\*p < 0.001, log-rank test; Bonferroni correction; n = 6 mice). (B) BALB/c mice were treated as in (A). 6 days after infection, 4 mice from each group were sacrificed and the lungs were isolated to determine the viral load by plaque assay. The viral titer of mice receiving mRNA encoding for Fc $\gamma$ RIV VHH-M2e VHH was significantly different compared to mice that received the control treatment (\*\*p < 0.001, Kruskal-Wallis; n = 4 mice). (C) C57BL/6 wild-type mice or C57BL/6 Fc $\gamma$ RIV<sup>-/-</sup> mice were i.t. instilled with 5  $\mu$ g mRNA encoding Fc $\gamma$ RIV VHH-M2e VHH or Fc $\gamma$ RIV VHH-RSVF VHH formulated in DOTAP/cholesterol particles. 4 h later, mice were challenged with 2 $\times$  LD<sub>50</sub> of A/X47 (H3N2) influenza virus. Body weight change (left) and survival (right) was monitored for 14 days. The mean relative changes in body weight together with their standard errors are represented. The survival rate of the wild-type mice receiving RiboBiFE encoding Fc $\gamma$ RIV VHH-M2e VHH was significantly different from wild-type mice treated with RiboBiFE encoding Fc $\gamma$ RIV VHH-RSVF VHH and Fc $\gamma$ RIV<sup>-/-</sup> mice treated with Fc $\gamma$ RIV VHH-M2e VHH and Fc $\gamma$ RIV VHH-RSVF VHH RiboBiFEs (\*\*p < 0.001, log-rank test; Bonferroni correction; n = 5 mice for the group treated with mRNA encoding Fc $\gamma$ RIV VHH-RSVF VHH and n = 6 for the group treated with mRNA encoding Fc $\gamma$ RIV VHH-M2e VHH).

otherwise lethal influenza challenge while Fc $\gamma$ RIV<sup>-/-</sup> mice, whereas control-treated wild-type and Fc $\gamma$ RIV<sup>-/-</sup> mice were not protected (Figure 4C).

Taken together, these data show that a single prophylactic administration of mRNA encoding two-domain construct Fc $\gamma$ RIV VHH-M2e VHH can protect mice against a potentially lethal influenza A virus challenge by specifically employing the mouse Fc $\gamma$ RIV.

## DISCUSSION

Previously, De Vlieger et al.<sup>16</sup> engineered a bispecific VHH fusion protein that selectively binds to and activates Fc $\gamma$ RIV present on innate immune cells with one moiety and binds to M2e present on influenza A virus infected cells with the other moiety. Here,

we added onto the findings reported by De Vlieger et al.<sup>16</sup> by formulating mRNA encoding the bispecific VHH fusion proteins, termed RiboBiFEs, into DOTAP/cholesterol particles. Through i.t. instillation of the mRNA-DOTAP/cholesterol particles, the bispecific VHH fusion proteins were produced *in situ* in the lungs, the specific site of virus infection in the murine influenza model, for a prolonged period of time as shown by ELISA on the BALF. We showed that i.t. administration of a single shot of RiboBiFEs 4 h before challenge with 2 $\times$  LD<sub>50</sub> of A/X47 (H3N2) influenza virus protects mice from excessive body weight loss and lethality caused by influenza virus infection. Furthermore, we confirmed the involvement of Fc $\gamma$ RIV engagement in the protection mediated by the RiboBiFEs. A notable improvement of the formulated mRNA delivery over the protein-based bi-specific VHH constructs

is the prolonged availability of the protective biologic in the lung compartment.

The most popular antibody-formats used in the clinic are full-size Igs of the IgG isotypes. These antibodies are produced mainly in mammalian cells since the heterotetrameric structure of such full-size Igs requires correct disulfide bridge formation and glycosylation for proper functioning.<sup>27,28</sup> Nearly 30 years ago also variable domain fragments of heavy-chain-only (VHH) Ab fragments were discovered. These VHHs are derived from heavy-chain-only antibodies of camelids and sharks and lack light chains.<sup>29,30</sup> Antibody fragments are also the basis of bispecific VHH that today form a huge family comprising a multitude of different formats.<sup>31–34</sup> Advantages of VHHs over conventional antibody formats are their outstanding solubility, stability, and excellent tissue penetration capacities. Moreover, due to their single-domain structure these VHHs can be easily formatted. Moreover, bispecific VHH are formed from a single construct. In contrast, two constructs are needed for a full-size Ab, one for the heavy chain and one for the light chain. Protein-based antibody therapeutics have been exploited in different branches of biomedical research. However, a wider implementation of protein-based antibodies is hampered by the high production cost and need for extensive purification processes. Alternative ways are now being explored, with mRNA coding for antibodies most recently emerging as a new genetic approach to deliver antibodies *in vivo*.<sup>11–14</sup> The main advantage of using mRNA encoding antibodies instead of the protein format is that the production of antibodies occurs in the body itself, for a prolonged period of time possibly in a cost-effective manner. We were able to detect bi-specific protein levels up to 48 h after instillation of mRNA encoding these bi-specific VHH's in the BAL fluid. To the contrary, De Vlieger et al.<sup>16</sup> could detect bi-specific VHHs until maximum 24 h after protein instillation.

For applications *in vivo*, specific formulation of mRNA is key. A number of nanoparticle carriers<sup>34,35</sup> have been proposed to increase the delivery efficiency of mRNA, protecting the mRNA against degradation by ubiquitous RNases and assisting in transfection of the intended target cells.<sup>36,37</sup> Here, mRNA encoding bi-specific VHH fusion proteins were formulated into DOTAP/cholesterol particles.<sup>26</sup> Through i.t. instillation of mRNA-DOTAP/cholesterol particles, the bi-specific VHH fusion proteins were *in situ* produced in the lungs, with a detectable presence of the therapeutic protein for at least 2 days. Previous reports<sup>5,38</sup> have shown that systemic delivery of mRNA nanoparticles composed of cationic lipids, such as DOTAP or 1,2-di-O-octadecenyl-3-trimethylammonium propane (DOTMA), can result in mRNA expression levels in the lungs and spleen. In two studies by Kranz et al.<sup>5</sup> and Rosigkeit et al.,<sup>38</sup> it was demonstrated that the organ selectivity between these organs depends on the particle surface charge and the helper lipid, with cationic mRNA lipoplexes composed with cholesterol holding a higher transfection efficiency in the lungs. Furthermore, they showed that this formulation was able to reach deep lung structures after intravenous (i.v.) administration, targeting endothelial cells, and epithelial cells, as well as lung-resident macrophages and dendritic cells. In our study, changing

the administration of the mRNA nanoparticles toward a pulmonary delivery route resulted in a specific cell targeting of alveolar macrophages and successful mRNA transfection in these cells.

With respect to the safety of this delivery approach, we observed that i.t. instillation of DOTAP/cholesterol mRNA nanoparticles resulted in a temporary influx of granulocytes in the lungs, combined with an increase in serum IL-6 cytokine levels. Importantly, these values were normalized within 24 h after administration. Furthermore, no other changes in levels of immune cells, nor increases in cytokine or chemokine levels, were observed. It should be noted that several steps could be taken that can potentially further improve the safety profile of the mRNA nanoparticles. The design and production of the nucleotide-modified mRNA construct can be fully optimized to eliminate innate immune activation to mRNA, for example by implementing more extensive purification methods for the removal of contaminants of double-stranded RNA (dsRNA) fragments. With respect to the immunotoxicity of lipid nanoparticles, this has been mainly attributed to their cationic nature.<sup>39,40</sup> Therefore, more clinically-advanced lipid formulations make use of a new generation of cationic lipids, referred to as ionizable aminolipids.<sup>41,42</sup> The acid dissociation constant (pKa) of these ionizable lipids gives them properties that allow them to form more stable complexes with mRNA at acidic pH, while potential “undesirable” immune-related events to the lipid formulation can be avoided, given their neutral charge at physiological pH.

In a prophylactic setting, we showed that a single shot of RiboBiFEs 4 h before challenge with  $2 \times LD_{50}$  of A/X47 (H3N2) influenza virus, protects mice from body weight loss and lethality caused by the influenza virus infection. Even more, the protection was mediated by FcγRIV engagement. The treatment described here can be seen as a disease-modulating treatment, meaning that the prophylactic treatment will not completely prevent infection but will induce an earlier clearance of the virus and therefore lower the morbidity. A potential advantage of this disease-modulating treatment includes that a moderate infection will take place and can prime an immune response against the viral pathogen. As a consequence, the immune system can act more effectively when a viral re-infection takes place. A disease-modulating treatment is an interesting option for people, which are at high risk of infection. By giving a single shot of the RiboBiFEs to this population, it might be possible to reduce the overall morbidity and the magnitude of the primary infection. Compared to a conventional influenza vaccination, the provided protection would be provided almost instantaneously and would be more transient.

## MATERIALS AND METHODS

### Cell Lines and Culture Conditions

Cells were cultured in Dulbecco's modified Eagle's medium (DMEM) supplemented with 10% of fetal calf serum, 2 mM of L-glutamine, 0.4 mM of Na-pyruvate, non-essential amino acids, 100 U/mL of penicillin, and 0.1 mg/mL of streptomycin at 37°C in a humidified

atmosphere containing 5% CO<sub>2</sub>. No full authentication was performed. Cells were tested negative for mycoplasma.

### Mice

All experiments were approved by and performed according to the guidelines of the animal ethical committee of Ghent University (Ethical application EC2017-092 and ECD 18/64). Female BALB/c mice aged 7–10 weeks were obtained from Charles River and *FcγRIV*<sup>-/-</sup> C57BL/6 mice were bred in-house. All animals were housed under specified pathogen-free conditions with food and water *ad libitum* and a 12/12-h light/dark cycle.

### mRNA

The coding information for the BiFE constructs were cloned into a pUC-plasmid vector containing a T7 promoter, 5' and 3' UTR of human β globulin, and a poly(A) tail. The plasmids were linearized with PstI (New England Biolabs, MA, USA) and purified using a PCR purification kit (Roche, Upper Bavaria, Germany). mRNA was produced with the T7 mMessage Machine Kit (Ambion, Austin, TX, USA) according to the manufacturer's instruction. N1-methylpseudouridine (TriLink, San Diego, CA, USA) was used in the transcription reactions instead of uridine. The *in vitro* transcribed mRNA was purified by lithium chloride precipitation and subsequently simultaneously capped and 2'-O-methylated to synthesize Cap 1 RNA from uncapped RNA using the ScriptCap m7G Capping System Kit together with the ScriptCap 2'-O-methyltransferase Kit (Ambion, Austin, TX, USA) according to the manufacturer's instruction. The capped *in vitro* transcribed mRNA was purified by lithium chloride precipitation. The mRNA constructs encoding for firefly luciferase or the fluorescent mCherry protein were purchased from TriLink (San Diego, CA, USA). These mRNAs are modified with 5-methoxyuridine, polyadenylated, and capped using a Clean-Cap method.

### mRNA Nanoparticle Preparation

The lipid-based nanoparticles composed with DOTAP and cholesterol were produced as described by Verbeke et al.<sup>26</sup> Lipids were purchased from Avanti Polar Lipids (Alabaster, AL, USA). Cationic liposomes of DOTAP/cholesterol (2:3 molar ratio) were prepared by transferring the appropriate amounts of lipids, dissolved in chloroform, into a round-bottom flask. For the cellular uptake study, 1 mol% of the total lipid amount was replaced by the lipophilic DiR fluorescent dye (Thermo Fisher Scientific). The chloroform was evaporated under nitrogen, after which the lipid film was rehydrated in HEPES buffer (20 mM, pH 7.4, Sigma-Aldrich) to obtain a final lipid concentration of 12.5 mM. The resulting cationic liposomes were sonicated in a bath sonicator (Branson Ultrasonics, Danbury, CT, USA). Next, liposomes were mixed with mRNA to obtain mRNA nanoparticles at a cationic lipid-to-mRNA (N/P) ratio of 3. mRNA nanoparticles for *in vivo* use were prepared in an isotonic HEPES buffer containing 5% glucose (Sigma-Aldrich). mRNA lipoplexes were subjected to a size quality control via Nanoparticle Tracking Analysis using the NanoSight LM10 (Malvern, Worcestershire, UK). These measurements were performed after incubating

the mRNA lipoplexes for 1 h at 37°C in either HEPES buffer or murine BALF. The murine BALF was collected by the protocol described by Van Hoecke et al.<sup>43</sup>

### In Vitro Transfection

HEK293T cells were plated 24 h before transfection in a 6-well plate at a density of 10<sup>6</sup> cells/well. The following day, cells were transfected with 5 μg of mRNA complexed with Lipofectamine RNAiMAX (Life Technologies, Ghent, Belgium) diluted in OptiMem to obtain a total volume of 300 μL. The transfection mix was added to the cells and cells were incubated at 37°C, 5% of CO<sub>2</sub> during a time period of 48 h.

### Western Blot

Supernatant of cells transfected with the mRNA constructs were separated by SDS-PAGE (15% acrylamide) under non-reducing conditions and His-tagged FcγRIV VHH-RSVF VHH and His-tagged FcγRIV VHH-M2e VHH protein were visualized by western blotting using anti-His (1,000× dilution; Bio-rad Abd Serotec, Cat. No. MCA1396) antibodies.

### ELISA

M2e-peptide ELISA was performed as described by De Filette et al.<sup>44</sup> Briefly, maxisorp 96-well microtiter plates (Thermo Fisher Scientific) were coated overnight with 100 ng M2e peptide (SLLTEVETPIRNEWGCRCNDSSD, corresponding to M2e of human H3N2 viruses) diluted in 0.1 M carbonate-bicarbonate buffer, pH 9.6. After overnight coating, wells were washed and blocked with 5% milk powder in phosphate buffered saline (PBS). Next, dilution series of the solution containing the VHHs (BALF or supernatant of cell culture) were added to the wells and incubated for 90 min. The bound VHHs were detected with mouse anti-histidine tag antibody (MCA1396, Abd Serotec) and horseradish peroxidase (HRP)-linked anti-mouse IgG (NXA931, GE Healthcare). Detection was done by adding 50 μL of TMB (Tetramethylbenzidine, BD OptETA) to every well; reactions were stopped by addition of 50 μL of 1M H<sub>2</sub>SO<sub>4</sub>. The absorbance was measured at 450 nm with an iMark Microplate Absorbance Reader (Bio Rad) using 655 nm as background measurement.

### In Vivo Expression and Distribution of mRNA Nanoparticles

Mice were anesthetized with isoflurane/air (Ecuphar, Oostkamp, Belgium) and i.t. instilled with mRNA DOTAP/cholesterol nanoparticles containing a dose of 5 μg mRNA (volume of 50 μL). For the bioluminescence imaging experiment, mRNA nanoparticles containing firefly luciferase encoding mRNA were used. 6 h after instillation of the mRNA nanoparticles, VivoGlo Luciferin-substrate (Promega) was administered intraperitoneally (i.p.) in a volume of 100 μL (33 mg/mL) per mouse. After 10 min, bioluminescence images were acquired using the IVIS lumina II system (PerkinElmer, Waltham, MA, USA), and quantitative analysis of the images was performed using the Living Image software (PerkinElmer). To evaluate the cellular uptake and cell-specific mRNA translation, we used mRNA nanoparticles containing the lipophilic DiR dye and mCherry mRNA. The fluorescent



signals of DiR (nanoparticle uptake) and the expression of mCherry protein (mRNA translation) were determined on single cell suspensions processed from complete lungs. At the indicated time points, mice were euthanized with an i.p. injection of 100  $\mu$ L Nembutal (Ceva Santé Animale, Libourne, France). The lungs were dissected and enzymatically dissociated with an enzymatic lung dissociation kit and gentleMACS dissociater (Miltenyi Biotec, Leiden, the Netherlands). Single cell suspensions were stained with a LIVE/DEAD Fixable Aqua dead cell stain (eBioscience) to exclude dead cells from analysis, incubated with Fc block (CD16/32) to block nonspecific FcR binding (BD Biosciences, Erembodegem, Belgium), and surface stained with monoclonal antibodies during 30 min at room temperature. The antibody panel to define different pulmonary immune subsets, including subsets of macrophages and dendritic cells, consists of CD45-BV421 (30-F11), CD11c-FITC (HL3), CD11b-PerCP-Cy5.5 (M1/70), CD24-BV711 (M1/69), CD64-APC (X54-5/7.1), and MHC-II-SB600 (M5/114.15.2) and was adopted from Knight et al.<sup>45</sup> After additional washing steps, the cells were analyzed on a four-laser fortessa (Becton Dickinson, San Jose, CA, USA), and data were analyzed using the FlowJo software (Treestar, Woodburn, OR, USA).

#### Absolute Bispecific Nanobody Titer Measurement

Mice were anesthetized with isoflurane/air (Ecuphar, Oostkamp, Belgium) and i.t. instilled with mRNA DOTAP/cholesterol nanoparticles containing a dose of 5  $\mu$ g mRNA (volume of 50  $\mu$ L) or with 50  $\mu$ g bispecific Fc $\gamma$ RIV VHH-M2e VHH fusion protein. 6, 24, or 48 h after instillation BALF was collected from the mice as described by Van Hoecke et al.<sup>43</sup> An M2e-peptide ELISA was performed on the BAL fluid as described above.

#### Cytokine Measurements

Serum was collected 6 or 24 h after i.t. instillation of the mRNA nanoparticles, and samples were stored at  $-80^{\circ}\text{C}$ . A panel of 13 cytokines, including IL-1 $\alpha$ , IL-1 $\beta$ , IL-6, IL-10, IL-12p70, IL-17A, IL-23, IL-27, monocyte chemoattractant protein 1 (MCP-1), interferon- $\beta$  (IFN- $\beta$ ), IFN- $\gamma$ , tumor necrosis factor alpha (TNF- $\alpha$ ), and granulocyte-macrophage colony-stimulating factor (GM-CSF), was quantified using a multiplex assay according to the manufacturer's instructions (LEGENDplex Mouse Inflammation Panel, Biolegend).

#### Challenge Experiment in Mice with H3N2

Mice were anesthetized with isoflurane and i.t. instilled with mRNA lipoplexes containing mRNA encoding Fc $\gamma$ RIV VHH-M2e VHH at a dose of 5  $\mu$ g mRNA. As controls, PBS or nanoparticles formulated with luciferase mRNA or a Fc $\gamma$ RIV VHH-RSVF VHH mRNA construct were administered. 4 h later, mice were anesthetized using isoflurane and challenged intranasally with  $2 \times \text{LD}_{50}$  of A/X47 (H3N2) influenza virus. Body weight loss was monitored for 14 days. When the body weight dropped below 75% of the initial body weight, mice were euthanized for ethical reasons.

#### Plaque Assay to Determine the Viral Titer

Complete lungs were harvested on day 6 after infection and homogenized in 1 mL of PBS using a sterile metal bead on the Mixer Mill

MM 200 (Retsch). Next, the lung homogenates were cleared by centrifuging at  $1,000 \times g$  for 10 min at  $4^{\circ}\text{C}$ . A serial dilution series of the cleared lung homogenates, made in serum-free DMEM medium, was added to a monolayer of Madin-Darby Canine Kidney (MDCK) cells in a 6-well plate (1 million cells per well). 1 h later, the cells were overlaid with an equal volume of 1.2% Avicel RC-591 (FMC Biopolymer) supplemented with 4  $\mu\text{g}/\text{mL}$  of L-1-tosylamido-2-phenylethyl chloromethyl ketone (TPCK)-treated trypsin (Sigma). Plates were incubated at  $37^{\circ}\text{C}$  in 5%  $\text{CO}_2$  for 3 days, after which the overlay was removed and cells were fixed with 4% paraformaldehyde. Viral plaques were stained using convalescent mouse anti-X47 serum followed by HRP-linked anti-mouse IgG (NXA931, GE Healthcare). After washing, the plaques were visualized with TrueBlue peroxidase substrate and counted (KPL, Gaithersburg, MD, USA).

#### Statistical Analyses

Statistical analyses were performed in GraphPad Prism 8 software. Statistical significance between survival rates was done by comparing Kaplan-Meier curves using the log-rank test and Bonferroni correction. Statistical significance between experimental groups was assessed using a Kruskal-Wallis test or by one-way ANOVA followed by Tukey's post hoc test, as indicated in the figure captions.

#### SUPPLEMENTAL INFORMATION

Supplemental Information can be found online at <https://doi.org/10.1016/j.omtn.2020.04.015>.

#### AUTHOR CONTRIBUTIONS

L.V.H., R.V., D.D.V., H.D., K.R., I.L., and X.S. planned the study. L.V.H., R.V., S.V.N., and O.K. performed the experiment. L.V.H. and R.V. wrote the manuscript and X.S. edited the manuscript. All authors reviewed the manuscript before submission.

#### CONFLICTS OF INTEREST

The authors declare no competing interests.

#### ACKNOWLEDGMENTS

L.V.H. is a junior assistant and B.S. a doctoral assistant of the Department of Biomedical Molecular Biology of Ghent University. Funding by the FWO Flanders (12E3916N) is acknowledged with gratitude. D.D.V. was supported by an FWO-sb fellowship and B.S. was also supported by FWO project VirEOS.

#### REFERENCES

1. Wolff, J.A., Malone, R.W., Williams, P., Chong, W., Acsadi, G., Jani, A., and Felgner, P.L. (1990). Direct gene transfer into mouse muscle *in vivo*. *Science* 247, 1465–1468.
2. Van Lint, S., Goyvaerts, C., Maenhout, S., Goethals, L., Disy, A., Benteyn, D., Pen, J., Bonehill, A., Heirman, C., Breckpot, K., and Thielemans, K. (2012). Preclinical evaluation of TriMix and antigen mRNA-based antitumor therapy. *Cancer Res.* 72, 1661–1671.
3. Circelli, L., Petrizzo, A., Tagliamonte, M., Heidenreich, R., Tornesello, M.L., Buonaguro, F.M., and Buonaguro, L. (2017). Immunological effects of a novel

- RNA-based adjuvant in liver cancer patients. *Cancer Immunol. Immunother.* 66, 103–112.
4. Scheel, B., Aulwurm, S., Probst, J., Stitz, L., Hoerr, I., Rammensee, H.G., Weller, M., and Pascolo, S. (2006). Therapeutic anti-tumor immunity triggered by injections of immunostimulating single-stranded RNA. *Eur. J. Immunol.* 36, 2807–2816.
  5. Kranz, L.M., Diken, M., Haas, H., Kreiter, S., Loquai, C., Reuter, K.C., Meng, M., Fritz, D., Vascotto, F., Hefesha, H., et al. (2016). Systemic RNA delivery to dendritic cells exploits antiviral defence for cancer immunotherapy. *Nature* 534, 396–401.
  6. Richner, J.M., Jagger, B.W., Shan, C., Fontes, C.R., Dowd, K.A., Cao, B., Himansu, S., Caine, E.A., Nunes, B.T.D., Medeiros, D.B.A., et al. (2017). Vaccine Mediated Protection Against Zika Virus-Induced Congenital Disease. *Cell* 170, 273–283.
  7. Bahl, K., Senn, J.J., Yuzhakov, O., Bulychiev, A., Brito, L.A., Hassett, K.J., Laska, M.E., Smith, M., Almarsson, Ö., Thompson, J., et al. (2017). Preclinical and Clinical Demonstration of Immunogenicity by mRNA Vaccines against H10N8 and H7N9 Influenza Viruses. *Mol. Ther.* 25, 1316–1327.
  8. Hoerr, I., Obst, R., Rammensee, H.G., and Jung, G. (2000). In vivo application of RNA leads to induction of specific cytotoxic T lymphocytes and antibodies. *Eur. J. Immunol.* 30, 1–7.
  9. Fotin-Mlecsek, M., Duchardt, K.M., Lorenz, C., Pfeiffer, R., Ojkić-Zrna, S., Probst, J., and Kallen, K.J. (2011). Messenger RNA-based vaccines with dual activity induce balanced TLR-7 dependent adaptive immune responses and provide antitumor activity. *J. Immunother.* 34, 1–15.
  10. Petsch, B., Schnee, M., Vogel, A.B., Lange, E., Hoffmann, B., Voss, D., Schlake, T., Thess, A., Kallen, K.J., Stitz, L., and Kramps, T. (2012). Protective efficacy of in vitro synthesized, specific mRNA vaccines against influenza A virus infection. *Nat. Biotechnol.* 30, 1210–1216.
  11. Tiwari, P.M., Vanover, D., Lindsay, K.E., Bawage, S.S., Kirschman, J.L., Bhosle, S., Lifland, A.W., Zurlo, C., and Santangelo, P.J. (2018). Engineered mRNA-expressed antibodies prevent respiratory syncytial virus infection. *Nat. Commun.* 9, 3999.
  12. Thran, M., Mukherjee, J., Pönisch, M., Fiedler, K., Thess, A., Mui, B.L., Hope, M.J., Tam, Y.K., Horscroft, N., Heidenreich, R., et al. (2017). mRNA mediates passive vaccination against infectious agents, toxins, and tumors. *EMBO Mol. Med.* 9, 1434–1447.
  13. Stadler, C.R., Bähr-Mahmud, H., Celik, L., Hebich, B., Roth, A.S., Roth, R.P., Karikó, K., Türeci, Ö., and Sahin, U. (2017). Elimination of large tumors in mice by mRNA-encoded bispecific antibodies. *Nat. Med.* 23, 815–817.
  14. Pardi, N., Scretto, A.J., Shan, X., Debonera, F., Glover, J., Yi, Y., Muramatsu, H., Ni, H., Mui, B.L., Tam, Y.K., et al. (2017). Administration of nucleoside-modified mRNA encoding broadly neutralizing antibody protects humanized mice from HIV-1 challenge. *Nat. Commun.* 8, 14630.
  15. Hamers-Casterman, C., Atarhouch, T., Muyldermans, S., Robinson, G., Hamers, C., Songa, E.B., Bendahman, N., and Hamers, R. (1993). Naturally occurring antibodies devoid of light chains. *Nature* 363, 446–448.
  16. De Vlioger, D., Hoffmann, K., Van Molle, I., Nerinckx, W., Van Hoecke, L., Ballegeer, M., Creytens, S., Remaut, H., Hengel, H., Schepens, B., and Saelens, X. (2019). Selective Engagement of FcγRIV by a M2e-Specific Single Domain Antibody Construct Protects Against Influenza A Virus Infection. *Front. Immunol.* 10, 2920.
  17. Fan, J., Liang, X., Horton, M.S., Perry, H.C., Citron, M.P., Heidecker, G.J., Fu, T.M., Joyce, J., Przysocki, C.T., Keller, P.M., et al. (2004). Preclinical study of influenza virus A M2 peptide conjugate vaccines in mice, ferrets, and rhesus monkeys. *Vaccine* 22, 2993–3003.
  18. Neiryneck, S., Deroo, T., Saelens, X., Vanlandschoot, P., Jou, W.M., and Fiers, W. (1999). A universal influenza A vaccine based on the extracellular domain of the M2 protein. *Nat. Med.* 5, 1157–1163.
  19. Slepishkin, V.A., Katz, J.M., Black, R.A., Gamble, W.C., Rota, P.A., and Cox, N.J. (1995). Protection of mice against influenza A virus challenge by vaccination with baculovirus-expressed M2 protein. *Vaccine* 13, 1399–1402.
  20. El Bakkouri, K., Descamps, F., De Filette, M., Smet, A., Festjens, E., Birkett, A., Van Rooijen, N., Verbeek, S., Fiers, W., and Saelens, X. (2011). Universal vaccine based on ectodomain of matrix protein 2 of influenza A: Fc receptors and alveolar macrophages mediate protection. *J. Immunol.* 186, 1022–1031.
  21. Ramos, E.L., Mitcham, J.L., Koller, T.D., Bonavia, A., Usner, D.W., Balaratnam, G., Fredlund, P., and Swiderek, K.M. (2015). Efficacy and safety of treatment with an anti-m2e monoclonal antibody in experimental human influenza. *J. Infect. Dis.* 211, 1038–1044.
  22. Pendzialek, J., Roose, K., Smet, A., Schepens, B., Kufer, P., Raum, T., Baeuerle, P.A., Muenz, M., Saelens, X., and Fiers, W. (2017). Bispecific T cell engaging antibody constructs targeting a universally conserved part of the viral M2 ectodomain cure and prevent influenza A virus infection. *Antiviral Res.* 141, 155–164.
  23. Williams, M., Bruhns, P., Saey, Y., Hammad, H., and Lambrecht, B.N. (2014). The function of Fcγ receptors in dendritic cells and macrophages. *Nat. Rev. Immunol.* 14, 94–108.
  24. Bruhns, P. (2012). Properties of mouse and human IgG receptors and their contribution to disease models. *Blood* 119, 5640–5649.
  25. Verbeke, R., Lentacker, I., Breckpot, K., Janssens, J., Van Calenbergh, S., De Smedt, S.C., and Dewitte, H. (2019). Broadening the Message: A Nanovaccine Co-loaded with Messenger RNA and α-GalCer Induces Antitumor Immunity through Conventional and Natural Killer T Cells. *ACS Nano* 13, 1655–1669.
  26. Verbeke, R., Lentacker, I., Wayteck, L., Breckpot, K., Van Bockstal, M., Descamps, B., Vanhove, C., De Smedt, S.C., and Dewitte, H. (2017). Co-delivery of nucleoside-modified mRNA and TLR agonists for cancer immunotherapy: Restoring the immunogenicity of immunosilent mRNA. *J. Control. Release* 266, 287–300.
  27. Jäger, V., Büssow, K., Wagner, A., Weber, S., Hust, M., Frenzel, A., and Schirrmann, T. (2013). High level transient production of recombinant antibodies and antibody fusion proteins in HEK293 cells. *BMC Biotechnol.* 13, 52.
  28. Walsh, G. (2014). Biopharmaceutical benchmarks 2014. *Nat. Biotechnol.* 32, 992–1000.
  29. Könnig, D., Zielonka, S., Grzeschik, J., Empting, M., Valldorf, B., Krah, S., Schröter, C., Sellmann, C., Hock, B., and Kolmar, H. (2017). Camelid and shark single domain antibodies: structural features and therapeutic potential. *Curr. Opin. Struct. Biol.* 45, 10–16.
  30. Hultberg, A., Temperton, N.J., Rosseels, V., Koenders, M., Gonzalez-Pajuelo, M., Schepens, B., Ibañez, L.I., Vanlandschoot, P., Schillemans, J., Saunders, M., et al. (2011). Llama-derived single domain antibodies to build multivalent, superpotent and broadened neutralizing anti-viral molecules. *PLoS ONE* 6, e17665.
  31. Choi, B.D., Kuan, C.T., Cai, M., Archer, G.E., Mitchell, D.A., Gedeon, P.C., Sanchez-Perez, L., Pastan, I., Bigner, D.D., and Sampson, J.H. (2013). Systemic administration of a bispecific antibody targeting EGFRvIII successfully treats intracerebral glioma. *Proc. Natl. Acad. Sci. USA* 110, 270–275.
  32. Fournier, P., and Schirrmacher, V. (2013). Bispecific antibodies and trispecific immunocytokines for targeting the immune system against cancer: preparing for the future. *BioDrugs* 27, 35–53.
  33. Zitron, I.M., Thakur, A., Norkina, O., Barger, G.R., Lum, L.G., and Mittal, S. (2013). Targeting and killing of glioblastoma with activated T cells armed with bispecific antibodies. *BMC Cancer* 13, 83.
  34. Kontermann, R.E. (2012). Dual targeting strategies with bispecific antibodies. *MAbs* 4, 182–197.
  35. Hajj, K.A., and Whitehead, K.A. (2017). Tools for translation: non-viral materials for therapeutic mRNA delivery. *Nat. Rev. Mater.* 2, 17056.
  36. Probst, J., Brechtel, S., Scheel, B., Hoerr, I., Jung, G., Rammensee, H.G., and Pascolo, S. (2006). Characterization of the ribonuclease activity on the skin surface. *Genet. Vaccines Ther.* 4, 4.
  37. Geall, A.J., Verma, A., Otten, G.R., Shaw, C.A., Hekele, A., Banerjee, K., Cu, Y., Beard, C.W., Brito, L.A., Krucker, T., et al. (2012). Nonviral delivery of self-amplifying RNA vaccines. *Proc. Natl. Acad. Sci. USA* 109, 14604–14609.
  38. Rosigkeit, S., Meng, M., Grunwitz, C., Gomes, P., Kreft, A., Hayduk, N., Heck, R., Pickert, G., Ziegler, K., Abassi, Y., et al. (2018). Monitoring Translation Activity of mRNA-Loaded Nanoparticles in Mice. *Mol. Pharm.* 15, 3909–3919.
  39. Lv, H., Zhang, S., Wang, B., Cui, S., and Yan, J. (2006). Toxicity of cationic lipids and cationic polymers in gene delivery. *J. Control. Release* 114, 100–109.
  40. Liu, L., Liu, Y., Xu, B., Liu, C., Jia, Y., Liu, T., Fang, C., Wang, W., Ren, J., He, Z., et al. (2018). Negative regulation of cationic nanoparticle-induced inflammatory toxicity

- through the increased production of prostaglandin E2 via mitochondrial DNA-activated Ly6C<sup>+</sup> monocytes. *Theranostics* 8, 3138–3152.
41. Akinc, A., Maier, M.A., Manoharan, M., Fitzgerald, K., Jayaraman, M., Barros, S., Ansell, S., Du, X., Hope, M.J., Madden, T.D., et al. (2019). The Onpattro story and the clinical translation of nanomedicines containing nucleic acid-based drugs. *Nat. Nanotechnol.* 14, 1084–1087.
  42. Sabnis, S., Kumarasinghe, E.S., Salerno, T., Mihai, C., Ketova, T., Senn, J.J., Lynn, A., Bulychev, A., McFadyen, I., Chan, J., et al. (2018). A Novel Amino Lipid Series for mRNA Delivery: Improved Endosomal Escape and Sustained Pharmacology and Safety in Non-human Primates. *Mol. Ther.* 26, 1509–1519.
  43. Van Hoecke, L., Job, E.R., Saelens, X., and Roose, K. (2017). Bronchoalveolar Lavage of Murine Lungs to Analyze Inflammatory Cell Infiltration. *J. Vis. Exp.* (123).
  44. De Filette, M., Martens, W., Roose, K., Deroo, T., Vervalle, F., Bentahir, M., Vandekerckhove, J., Fiers, W., and Saelens, X. (2008). An influenza A vaccine based on tetrameric ectodomain of matrix protein 2. *J. Biol. Chem.* 283, 11382–11387.
  45. Knight, F.C., Gilchuk, P., Kumar, A., Becker, K.W., Sevimli, S., Jacobson, M.E., Suryadevara, N., Wang-Bishop, L., Boyd, K.L., Crowe, J.E., Jr., et al. (2019). Mucosal Immunization with a pH-Responsive Nanoparticle Vaccine Induces Protective CD8<sup>+</sup> Lung-Resident Memory T Cells. *ACS Nano* 13, 10939–10960.

**OMTN, Volume 20**

**Supplemental Information**

**mRNA Encoding a Bispecific Single  
Domain Antibody Construct Protects  
against Influenza A Virus Infection in Mice**

**Lien Van Hoecke, Rein Verbeke, Dorien De Vlieger, Heleen Dewitte, Kenny Roose, Sharon Van Nevel, Olga Krysko, Claus Bachert, Bert Schepens, Ine Lentacker, and Xavier Saelens**



## Supplementary information

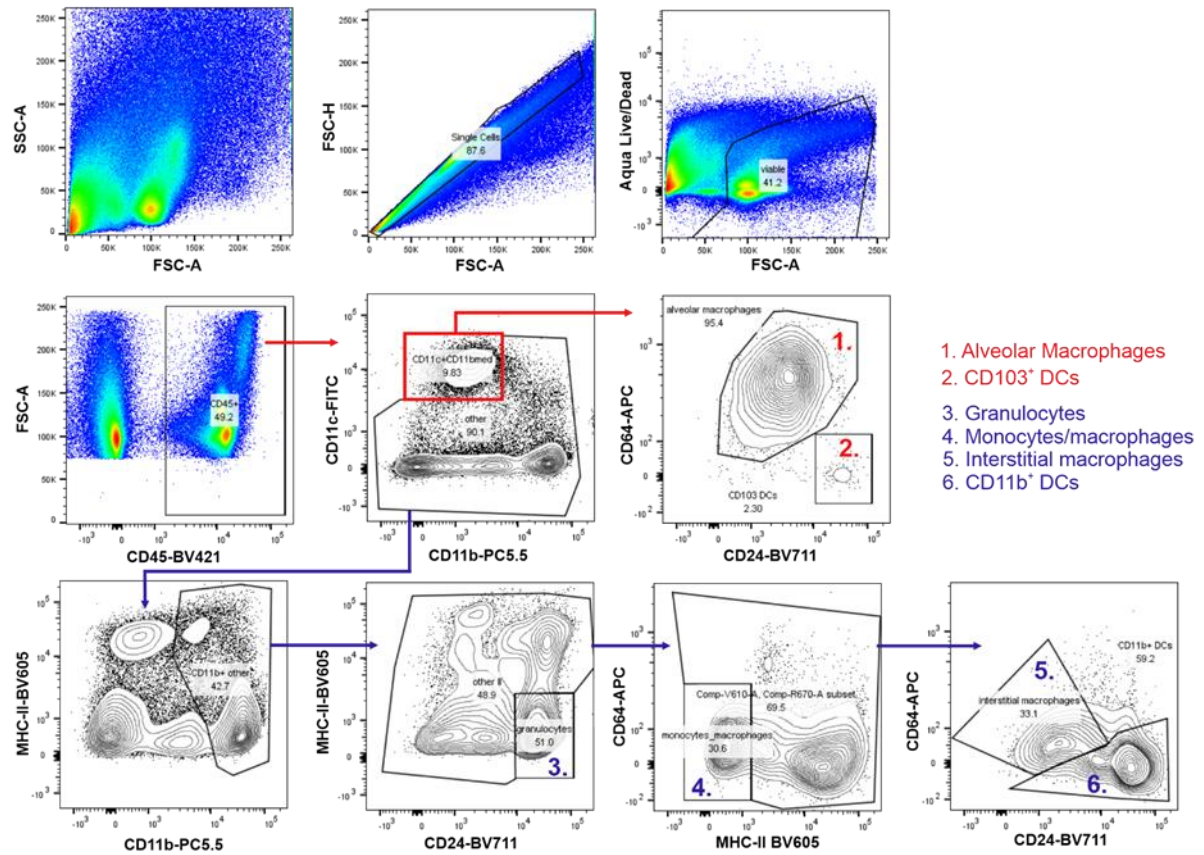


**Figure S1.** Gating strategy for flow cytometric analysis of the nanoparticle uptake (DiR signal) and mCherry mRNA expression in pulmonary innate immune cells after intratracheal instillation of DOTAP/cholesterol nanoparticles containing 5  $\mu$ g mCherry mRNA and fluorescent DiR dye. The gating strategy was based on a report from Knight *et al*<sup>27</sup>. Cells were selected on singlets (FSC-A, FSC-H) and viability (Aqua Live/Dead stain). Within the immune cell population (CD45-BV421), cell subsets were subsequently identified based on the surface markers: CD11c-FITC, CD11b-PC5.5., CD64-APC, CD24-BV711 and MHC-II-BV605. In each cell subset, uptake of nanoparticles (DiR-APC750) and mCherry mRNA expression (mCherry-Y610) were evaluated.

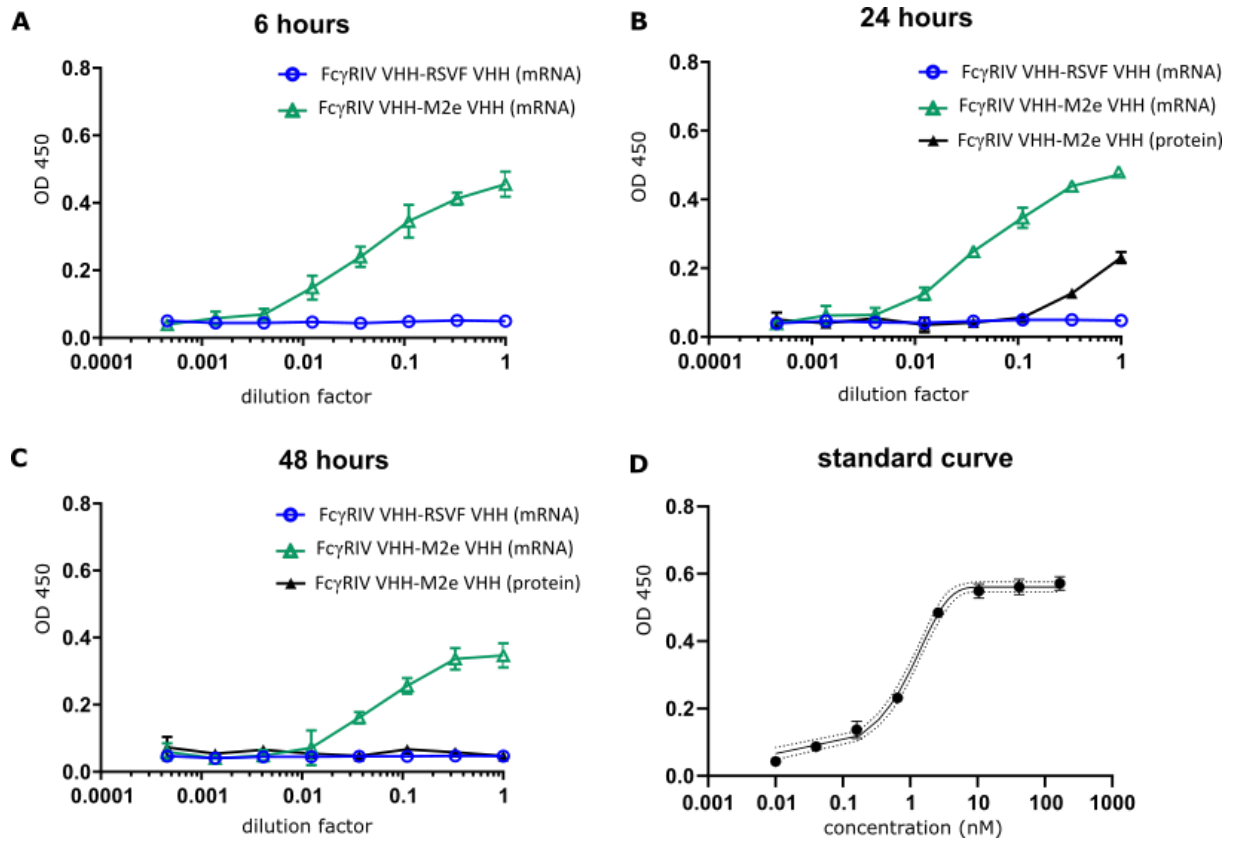


**Figure S2. A, B and C.** Five  $\mu\text{g}$  of Fc $\gamma$ RIV VHH-M2e VHH or Fc $\gamma$ RIV VHH-RSVF VHH (irrelevant mRNA) formulated in DOTAP/cholesterol particles or 50  $\mu\text{g}$  Fc $\gamma$ RIV VHH-M2e VHH protein was instilled i.t. in BALB/c mice. Six, 24 or 48 hours after instillation, BALF was isolated and cells were removed from the BALF and the ability of His<sub>6</sub>-tagged proteins to bind to M2e was investigated in a peptide ELISA. **D.** Standard curve of binding between M2e and the M2e VHH. This standard curve was used to calculate absolute concentration of the M2e VHH in the BALF.